

# Some computational results for $\mathbf{P}_1 - P_1$ and $\mathbf{P}_2 - P_1$ Trace FEM for the surface Stokes problem

Alexander Zhiliakov\*

July 16, 2019

## Contents

<b>1 Preliminaries</b>	<b>2</b>
1.1 Bilinear forms and matrices . . . . .	2
1.2 Quadratures for bilinear forms . . . . .	3
1.3 Error computation . . . . .	6
<b>2 Convergence results</b>	<b>6</b>
2.1 Manufactured solution . . . . .	6
2.2 $P_2 - P_1$ Trace FEM . . . . .	8
2.2.1 Inconsistent penalty formulation . . . . .	8
2.2.2 Consistent penalty formulation . . . . .	9
<b>3 Inf-sup stability: pressure Schur complement generalized eigenvalues</b>	<b>9</b>
3.1 Solution description . . . . .	9
3.2 Dependency of the spectrum on the mesh size . . . . .	10
3.3 Sensitivity of the spectrum to levelset shifts . . . . .	12

---

\*Department of Mathematics, University of Houston, Houston, Texas 77204 (alex@math.uh.edu).

# 1 Preliminaries

**1.1 Bilinear forms and matrices.** We set  $n_{\mathbf{A}}$  to be the number of velocity d.o.f. and  $n_{\mathbf{S}}$  to be the number of pressure d.o.f. Vector stiffness, divergence, pressure mass, normal stabilization, and full stabilization matrices resulting from Trace FEM discretization of the surface Stokes problem [2] are defined via

$$\begin{aligned}
 \langle \mathbf{A} \vec{\mathbf{u}}, \vec{\mathbf{v}} \rangle &\approx \int_{\Gamma} \left( 2 E_{s,\Gamma}(\mathbf{u}) : E_{s,\Gamma}(\mathbf{v}) + \mathbf{u} \cdot \mathbf{v} + \tau (\mathbf{u} \cdot \mathbf{n}_{\Gamma}) (\mathbf{v} \cdot \mathbf{n}_{\Gamma}) \right) ds \\
 &\quad + \rho_u \int_{\Omega_h^{\Gamma}} \frac{\partial \mathbf{u}}{\partial \mathbf{n}_{\Gamma}} \cdot \frac{\partial \mathbf{v}}{\partial \mathbf{n}_{\Gamma}} dx, \quad \mathbf{A} \in \mathbb{R}^{n_{\mathbf{A}} \times n_{\mathbf{A}}}, \\
 \langle \mathbf{B} \vec{\mathbf{u}}, \vec{\mathbf{q}} \rangle &\approx \int_{\Gamma} \nabla_{\Gamma} q \cdot \mathbf{u} ds, \quad \mathbf{B} \in \mathbb{R}^{n_{\mathbf{S}} \times n_{\mathbf{A}}}, \\
 \langle \mathbf{M}_0 \vec{\mathbf{p}}, \vec{\mathbf{q}} \rangle &\approx \int_{\Gamma} p q ds, \quad \mathbf{M}_0 \in \mathbb{R}^{n_{\mathbf{S}} \times n_{\mathbf{S}}}, \\
 \langle \mathbf{C}_n \vec{\mathbf{p}}, \vec{\mathbf{q}} \rangle &\approx \rho_p \int_{\Omega_h^{\Gamma}} \frac{\partial p}{\partial \mathbf{n}_{\Gamma}} \frac{\partial q}{\partial \mathbf{n}_{\Gamma}} dx, \quad \mathbf{C}_n \in \mathbb{R}^{n_{\mathbf{S}} \times n_{\mathbf{S}}}, \\
 \langle \mathbf{C}_{\text{full}} \vec{\mathbf{p}}, \vec{\mathbf{q}} \rangle &\approx \rho_p \int_{\Omega_h^{\Gamma}} \nabla p \cdot \nabla q dx, \quad \mathbf{C}_{\text{full}} \in \mathbb{R}^{n_{\mathbf{S}} \times n_{\mathbf{S}}},
 \end{aligned} \tag{1}$$

respectively. We use notations as in [2], in particular,  $\Omega_h^{\Gamma}$  is the domain consisting of tetrahedra cut by the surface  $\Gamma := \{\mathbf{x} \in \mathbb{R}^3 : \phi(\mathbf{x}) = 0\}$ . Here  $\vec{\mathbf{u}}$  denotes a vector of d.o.f. corresponding to a FE interpolant  $\mathbf{u}$  (analogously for  $\vec{\mathbf{p}}$  and  $p$ ). See (5) and (6) for the computational details. Mesh-dependent parameters  $\tau$ ,  $\rho_u$ , and  $\rho_p$  are chosen to be proportional to some power of  $h :=$  the typical mesh size for tetrahedra from  $\Omega_h^{\Gamma}$ .  $\Gamma$  is chosen either as the unit sphere or torus,  $\Gamma = \Gamma_{\text{sph}}$  or  $\Gamma = \Gamma_{\text{tor}}$  (see Figure 1). The background domain is chosen as a cube  $\Omega := (-5/3, 5/3)^3$ .

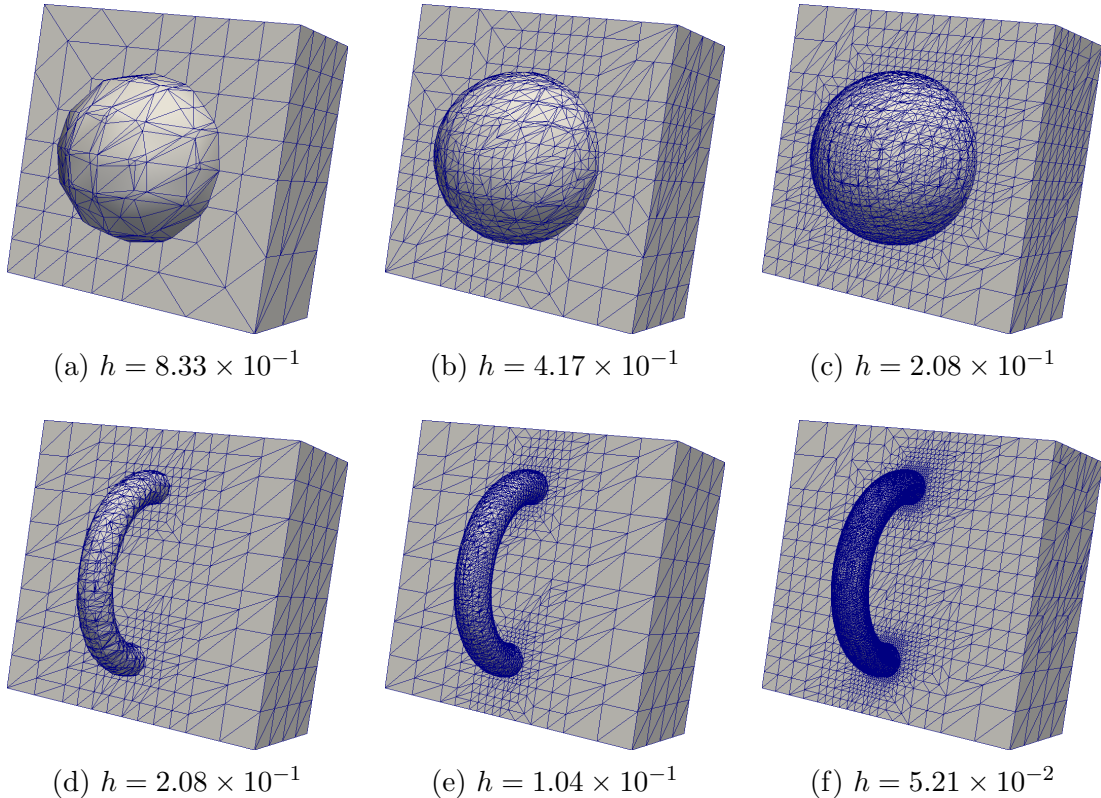


Figure 1: First three mesh levels for  $\Gamma_{\text{sph}}$  (top) and  $\Gamma_{\text{tor}}$  (bottom)

**1.2 Quadratures for bilinear forms.** We denote by  $P_h^n \subset \bar{P}_h^n$  spaces of continuous and discontinuous nodal  $P_n$  interpolants defined on  $\Omega_\Gamma^h$ , respectively. For a function  $f$ ,  $I_h^n(f) \in P_h^n$  is the corresponding interpolant; we will use the notation  $f_h^n$  to emphasize that  $f_h^n \in P_h^n$  and  $f_h^n$  approximates  $f$  in some sense, but  $I_h^n(f) \neq f_h^n$ .

We set

$$\Gamma_h^n := \{\mathbf{x} \in \mathbb{R}^3 : (I_h^n(\phi))(\mathbf{x}) = 0\}, \quad (2)$$

$$\mathbf{n}_{\Gamma_h^n} = \frac{\nabla I_h^n(\phi)}{\|\nabla I_h^n(\phi)\|} \notin \bar{P}_h^m \text{ for any } m \text{ if } n > 1. \quad (3)$$

Note that  $\Gamma_h^n$  is a continuous piecewise  $P_n$  surface in  $\Omega_\Gamma^h$ , and  $\Gamma_h^n \neq I_h^n(\Gamma)$ . The unit normal  $\mathbf{n}_{\Gamma_h^n}$  is not a rational function; it is continuous in  $T \in \Omega_\Gamma^h$  and discontinuous on faces. We also define

$$\Gamma_{h/m}^{2 \rightarrow 1} := \{\mathbf{x} \in \mathbb{R}^3 : (I_{h/m}^1(I_h^2(\phi)))(\mathbf{x}) = 0\}. \quad (4)$$

Note that  $I_{h/2}^1(I_h^2(\phi)) = I_{h/2}^1(\phi)$  (since in order to build both  $I_{h/2}^1$  and  $I_h^2$  the same values of  $\phi$  are used), and  $I_{h/m}^1(I_h^2(\phi)) \neq I_{h/m}^1(\phi)$  for  $m > 2$ . Thus we have  $\Gamma_{h/2}^{2 \rightarrow 1} = \Gamma_{h/2}^1$ , and  $\Gamma_{h/m}^{2 \rightarrow 1} \neq \Gamma_{h/m}^1$  for  $m > 2$ . We refer to Figures 2 and 3.

We implemented two options for the matrix assembly (1). The first one is

$$\begin{aligned} \langle \mathbf{A} \vec{\mathbf{u}}, \vec{\mathbf{v}} \rangle &= \int_{\Gamma_{h/m}^{2 \rightarrow 1}}^5 (2 E_{s, \Gamma_h^2}(\mathbf{u}) : E_{s, \Gamma_h^2}(\mathbf{v}) + \mathbf{u} \cdot \mathbf{v} + \tau (\mathbf{u} \cdot \mathbf{n}_{\Gamma_h^2})(\mathbf{v} \cdot \mathbf{n}_{\Gamma_h^2})) \, ds \\ &\quad + \rho_u \int_{\Omega_h^\Gamma}^5 \frac{\partial \mathbf{u}}{\partial \mathbf{n}_{\Gamma_h^2}} \cdot \frac{\partial \mathbf{v}}{\partial \mathbf{n}_{\Gamma_h^2}} \, d\mathbf{x}, \quad \mathbf{A} \in \mathbb{R}^{n_A \times n_A}, \\ \langle \mathbf{B} \vec{\mathbf{u}}, \vec{\mathbf{q}} \rangle &= \int_{\Gamma_{h/m}^{2 \rightarrow 1}}^5 \nabla_{\Gamma_h^2} q \cdot \mathbf{u} \, ds, \quad \mathbf{B} \in \mathbb{R}^{n_S \times n_A}, \\ \langle \mathbf{M}_0 \vec{\mathbf{p}}, \vec{\mathbf{q}} \rangle &= \int_{\Gamma_{h/m}^{2 \rightarrow 1}}^5 p q \, ds, \quad \mathbf{M}_0 \in \mathbb{R}^{n_S \times n_S}, \\ \langle \mathbf{C}_n \vec{\mathbf{p}}, \vec{\mathbf{q}} \rangle &= \rho_p \int_{\Omega_h^\Gamma}^5 \frac{\partial p}{\partial \mathbf{n}_{\Gamma_h^2}} \frac{\partial q}{\partial \mathbf{n}_{\Gamma_h^2}} \, d\mathbf{x}, \quad \mathbf{C}_n \in \mathbb{R}^{n_S \times n_S}, \\ \langle \mathbf{C}_{\text{full}} \vec{\mathbf{p}}, \vec{\mathbf{q}} \rangle &= \rho_p \int_{\Omega_h^\Gamma}^5 \nabla p \cdot \nabla q \, d\mathbf{x}, \quad \mathbf{C}_{\text{full}} \in \mathbb{R}^{n_S \times n_S}. \end{aligned} \quad (5)$$

- $\int_{\Gamma_{h/m}^{2 \rightarrow 1}}^5 \cdot \, ds$  denotes a composite quadrature rule that is exact for  $\bar{P}_h^5(\Gamma_{h/m}^{2 \rightarrow 1})$ , i.e. this quadrature is exact for piecewise polynomials up to degree 5 on each triangular patch  $\gamma \in \Gamma_{h/m}^{2 \rightarrow 1}$ ,
- $\int_{\Omega_h^\Gamma}^5 \cdot \, d\mathbf{x}$  denotes a composite quadrature rule that is exact for  $\bar{P}_h^5(\Omega_h^\Gamma)$ , i.e. this quadrature is exact for piecewise polynomials up to degree 5 on each tetrahedron  $T \in \Omega_h^\Gamma$ ,
- $E_{s, \Gamma_h^2}$  and  $\nabla_{\Gamma_h^2}$  are defined as their continuous analogues with  $\mathbf{n}_\Gamma$  in  $\mathbf{P}_\Gamma$  replaced with  $\mathbf{n}_{\Gamma_h^2}$ .

The second option is

$$\begin{aligned}
\langle \mathbf{A} \vec{\mathbf{u}}, \vec{\mathbf{v}} \rangle &= \int_{\Gamma_{h/m}^{2 \rightarrow 1}}^5 \left( 2 E_{s, \Gamma_{h/m}^{2 \rightarrow 1}}(\mathbf{u}) : E_{s, \Gamma_{h/m}^{2 \rightarrow 1}}(\mathbf{v}) + \mathbf{u} \cdot \mathbf{v} + \tau (\mathbf{u} \cdot \mathbf{n}_{\Gamma_h^2}) (\mathbf{v} \cdot \mathbf{n}_{\Gamma_h^2}) \right) ds \\
&\quad + \rho_u \int_{\Omega_h^\Gamma} \frac{\partial \mathbf{u}}{\partial \mathbf{n}_{\Gamma_h^2}} \cdot \frac{\partial \mathbf{v}}{\partial \mathbf{n}_{\Gamma_h^2}} d\mathbf{x}, \quad \mathbf{A} \in \mathbb{R}^{n_A \times n_A}, \\
\langle \mathbf{B} \vec{\mathbf{u}}, \vec{\mathbf{q}} \rangle &= \int_{\Gamma_{h/m}^{2 \rightarrow 1}}^5 \nabla_{\Gamma_{h/m}^{2 \rightarrow 1}} q \cdot \mathbf{u} ds, \quad \mathbf{B} \in \mathbb{R}^{n_S \times n_A}, \\
\langle \mathbf{M}_0 \vec{\mathbf{p}}, \vec{\mathbf{q}} \rangle &= \int_{\Gamma_{h/m}^{2 \rightarrow 1}}^5 p q ds, \quad \mathbf{M}_0 \in \mathbb{R}^{n_S \times n_S}, \\
\langle \mathbf{C}_n \vec{\mathbf{p}}, \vec{\mathbf{q}} \rangle &= \rho_p \int_{\Omega_h^\Gamma} \frac{\partial p}{\partial \mathbf{n}_{\Gamma_h^2}} \frac{\partial q}{\partial \mathbf{n}_{\Gamma_h^2}} d\mathbf{x}, \quad \mathbf{C}_n \in \mathbb{R}^{n_S \times n_S}, \\
\langle \mathbf{C}_{\text{full}} \vec{\mathbf{p}}, \vec{\mathbf{q}} \rangle &= \rho_p \int_{\Omega_h^\Gamma} \nabla p \cdot \nabla q d\mathbf{x}, \quad \mathbf{C}_{\text{full}} \in \mathbb{R}^{n_S \times n_S}.
\end{aligned} \tag{6}$$

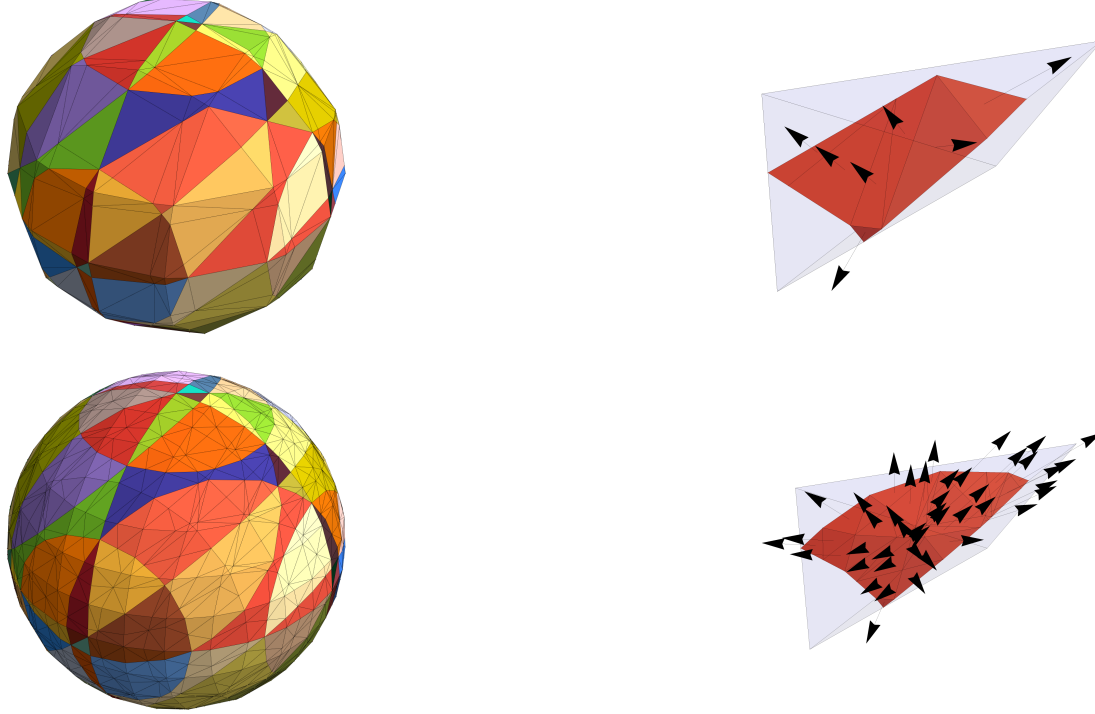


Figure 2:  $\Gamma = \Gamma_{\text{sph}}$ ,  $\phi(\mathbf{x}) = \|\mathbf{x}\|^2 - 1$ ,  $h = 8.33 \times 10^{-1}$ . Top-left: triangular patches  $\gamma \in \Gamma_{h/2}^{2 \rightarrow 1} = \Gamma_{h/2}^1$  (different color corresponds to a different tetrahedron  $T \in \Omega_h^\Gamma$ ). Top-right: a patch  $\gamma$  and its normals. Bottom-left and bottom-right: same for  $\Gamma_{h/4}^{2 \rightarrow 1} = \Gamma_{h/4}^1$ . **Note that since  $\phi \in P^2$ , we have that  $\Gamma_{h/m}^{2 \rightarrow 1} = \Gamma_{h/m}^1 \rightarrow \Gamma$  as  $m \rightarrow \infty$  even for fixed  $h$**

For both formulations (5) and (6) the loading vectors for moments and continuity equations are approximated

as

$$\begin{aligned}\mathbf{f}_i &= \int_{\Gamma_{h/m}^{2 \rightarrow 1}}^5 \mathbf{f} \cdot \phi_i \, ds, \quad i = 1, 2, \dots, n_{\mathbf{A}}, \\ \mathbf{g}_i &= - \int_{\Gamma_{h/m}^{2 \rightarrow 1}}^5 g \phi_i \, ds, \quad i = 1, 2, \dots, n_{\mathbf{S}},\end{aligned}\tag{7}$$

respectively. Here  $\phi_i$  and  $\phi_i$  are vector and scalar Lagrange basis functions defined on  $\Omega_h^\Gamma$ .



Figure 3:  $\Gamma = \Gamma_{\text{sph}}$ ,  $\phi(\mathbf{x}) = \|\mathbf{x}\|^{1/2} - 1$ ,  $h = 8.33 \times 10^{-1}$ . Left: triangular patches  $\gamma \in \Gamma_{h/2}^1$  (different color corresponds to a different tetrahedron  $T \in \Omega_h^\Gamma$ ). Right: same for  $\Gamma_{h/4}^{2 \rightarrow 1} \neq \Gamma_{h/4}^1$ . **Note that since**  $\phi \notin \bar{P}_h^2$ , **we have that**  $\Gamma_{h/m}^{2 \rightarrow 1} \neq \Gamma_{h/m}^1$  **for**  $m > 2$ , **and**  $\Gamma_{h/m}^{2 \rightarrow 1} \rightarrow \Gamma_h^2 \neq \Gamma$  **as**  $m \rightarrow \infty$  **for fixed**  $h$

As in [1], we refer to (1) as **inconsistent formulation**. We also consider the same formulation as in (1) but with the first term  $\mathbf{A}_s$  in the definition of  $\mathbf{A}$  changed as

$$\langle \mathbf{A}_s \vec{\mathbf{u}}, \vec{\mathbf{v}} \rangle \approx \int_{\Gamma} 2(E_{s,\Gamma}(\mathbf{u}) - (\mathbf{u} \cdot \mathbf{n}_{\Gamma}) \mathbf{H}_{\Gamma}) : (E_{s,\Gamma}(\mathbf{v}) - (\mathbf{v} \cdot \mathbf{n}_{\Gamma}) \mathbf{H}_{\Gamma}) \, ds, \tag{8}$$

where the shape operator is defined as  $\mathbf{H}_{\Gamma} := \nabla_{\Gamma} \mathbf{n}_{\Gamma} := \mathbf{P}_{\Gamma} \nabla \mathbf{n}_{\Gamma}^e \mathbf{P}_{\Gamma}$ ,  $\mathbf{H}_{\Gamma} : \mathcal{O}(\Gamma) \rightarrow \mathbb{R}^3$ . We refer to (8) as **consistent formulation**.

Similarly to (5) and (6), we consider two discretizations of (8):

$$\langle \mathbf{A}_s \vec{\mathbf{u}}, \vec{\mathbf{v}} \rangle = \int_{\Gamma_{h/m}^{2 \rightarrow 1}}^5 2(E_{s,\Gamma_h^2}(\mathbf{u}) - (\mathbf{u} \cdot \mathbf{n}_{\Gamma_h^2}) \mathbf{H}_{\Gamma_h^2}) : (E_{s,\Gamma_h^2}(\mathbf{v}) - (\mathbf{v} \cdot \mathbf{n}_{\Gamma_h^2}) \mathbf{H}_{\Gamma_h^2}) \, ds \tag{9}$$

and

$$\langle \mathbf{A}_s \vec{\mathbf{u}}, \vec{\mathbf{v}} \rangle = \int_{\Gamma_{h/m}^{2 \rightarrow 1}}^5 2(E_{s,\Gamma_{h/m}^{2 \rightarrow 1}}(\mathbf{u}) - (\mathbf{u} \cdot \mathbf{n}_{\Gamma_{h/m}^{2 \rightarrow 1}}) \mathbf{H}_{\Gamma_h^2}) : (E_{s,\Gamma_{h/m}^{2 \rightarrow 1}}(\mathbf{v}) - (\mathbf{v} \cdot \mathbf{n}_{\Gamma_{h/m}^{2 \rightarrow 1}}) \mathbf{H}_{\Gamma_h^2}) \, ds. \tag{10}$$

Note that  $\mathbf{n}_{\Gamma} = \nabla \phi / \|\nabla \phi\|$  is defined in  $\mathcal{O}(\Gamma)$ , so  $\nabla \mathbf{n}_{\Gamma}$  makes sense and

$$\nabla \mathbf{n}_{\Gamma} = \left( \mathbf{I} - \frac{\nabla \phi \nabla \phi^T}{\|\nabla \phi\|^2} \right) \frac{\nabla^2 \phi}{\|\nabla \phi\|} = \mathbf{P}_{\Gamma} \frac{\nabla^2 \phi}{\|\nabla \phi\|}.$$

If  $\mathbf{n}_{\Gamma} = \mathbf{n}_{\Gamma}^e$ , one gets

$$\mathbf{H}_{\Gamma} = \mathbf{P}_{\Gamma} \frac{\nabla^2 \phi}{\|\nabla \phi\|} \mathbf{P}_{\Gamma}. \tag{11}$$

Thus we define  $\mathbf{H}_{\Gamma_h^2}$  to be as in (11) but with  $\phi$  replaced with  $I_h^2(\phi)$ , i.e.

$$\mathbf{H}_{\Gamma_h^2} := \mathbf{P}_{\Gamma_h^2} \frac{\nabla^2 I_h^2(\phi)}{\|\nabla I_h^2(\phi)\|} \mathbf{P}_{\Gamma_h^2}. \quad (12)$$

Indeed, computation of  $\mathbf{H}_{\Gamma_h^2}$  requires Hessians of shape functions.

Depending on the choice of  $\phi$ , we may or may not have  $\mathbf{n}_\Gamma = \mathbf{n}_\Gamma^e$ . Note that the choice  $\phi = d$  is sufficient for this, but not necessary. Consider this choices of  $\phi$  for  $\Gamma_{\text{sph}}$ :

1.  $\phi_1(\mathbf{x}) = \|\mathbf{x}\| - 1 = d(\mathbf{x})$ ,  $\nabla\phi_1/\|\nabla\phi_1\| = \mathbf{n}_\Gamma^e$ ,
2.  $\phi_2(\mathbf{x}) = \|\mathbf{x}\|^2 - 1 \in P^2$ ,  $\nabla\phi_2/\|\nabla\phi_2\| = \nabla\phi_1/\|\nabla\phi_1\| = \mathbf{n}_\Gamma^e$ ,
3.  $\phi_3(\mathbf{x}) = e^{\phi_2(\mathbf{x})} x^2 + y^2 + z^2 - 1$ ,  $\nabla\phi_3/\|\nabla\phi_3\| \neq \mathbf{n}_\Gamma^e$ , i.e.  $\nabla\phi_3/\|\nabla\phi_3\| = \mathbf{n}_\Gamma$  only on  $\Gamma_{\text{sph}}$ .

As for the case 2: note that if  $\phi$  is piecewise quadratic in  $\Omega_h^\Gamma$  and defines a normal that is equal to its extension, then  $\mathbf{H}_{\Gamma_h^2} = \mathbf{H}_\Gamma$ , i.e. the approximation is **exact**.

For the approach (6), there is also an option to approximate  $\mathbf{H}$  as  $\mathbf{P}_{\Gamma_{h/m}^{2 \rightarrow 1}} \frac{\nabla^2 I_h^2(\phi)}{\|\nabla I_h^2(\phi)\|} \mathbf{P}_{\Gamma_{h/m}^{2 \rightarrow 1}}$  since we build  $\mathbf{P}_{\Gamma_{h/m}^{2 \rightarrow 1}}$  anyway. We chose to use (12) for both (5) and (6).

**1.3 Error computation.** Note that  $\mathbb{H}^1(\Gamma)$ -error (for e.g.  $\mathbf{P}_2 - P_1$  FE) can be cheaply approximated as  $\langle \mathbf{w}, \mathbf{A}_s \mathbf{w} \rangle^{1/2}$  where  $\mathbf{w} :=$  vector of d.o.f. corresponding to  $\mathbf{P}_h^2$  interpolant  $I_h^2(\mathbf{u}^e) - \mathbf{u}_h$ ,  $\mathbf{A}_s :=$  matrix corresponding to the first term of  $\mathbf{A}$  in (6). Thus the errors are approximated as

$$\begin{aligned} \|\mathbf{u} - \mathbf{u}_h\|_{\mathbb{H}^1(\Gamma)} &= \|I_h^k(\mathbf{u}^e) - \mathbf{u}_h\|_{\mathbb{H}^1(\Gamma_{h/m}^{2 \rightarrow 1})} + O(h^k), \\ \|\mathbf{u} - \mathbf{u}_h\|_{\mathbb{L}^2(\Gamma)} &= \|I_h^k(\mathbf{u}^e) - \mathbf{u}_h\|_{\mathbb{L}^2(\Gamma_{h/m}^{2 \rightarrow 1})} + O(h^{k+1}), \\ \|p - p_h\|_{\mathbb{L}^2(\Gamma)} &= \|I_h^1(p^e) - p_h\|_{\mathbb{L}^2(\Gamma_{h/m}^{2 \rightarrow 1})} + O(h^2) \end{aligned} \quad (13)$$

for  $m > 1$ . Here  $k = 1$  for  $\mathbf{P}_1 - P_1$  FEM and  $k = 2$  for  $\mathbf{P}_2 - P_1$ . For consistent penalty approach matrix  $\mathbf{A}_s$  is computed as in (9) or (10).

## 2 Convergence results

**2.1 Manufactured solution.** We solve model problem from [2, p. 20],  $\Gamma = \Gamma_{\text{sph}}$ <sup>1</sup>. We set

$$\tilde{\mathbf{u}}(x, y, z) := (-z^2, y, x)^T, \quad \tilde{p}(x, y, z) := x y^2 + z, \quad \phi(\mathbf{x}) := \|\mathbf{x}\|^2 - 1. \quad (14)$$

The exact solution on the unit sphere is chosen as

$$\mathbf{u} := \mathbf{P}_\Gamma \tilde{\mathbf{u}}^e, \quad p := \tilde{p}^e. \quad (15)$$

Thus we have  $\int_\Gamma p \, d\mathbf{x} = 0$ ,  $p \equiv p^e$ ,  $\mathbf{u} \equiv \mathbf{u}^e$  in  $\mathcal{O}(\Gamma)$ , and  $\mathbf{u}$  is a tangential field. Note that for our choice of  $\phi$  in (14) we have

$$\mathbf{n}_{\Gamma_h^2} = \mathbf{n}_\Gamma^e \text{ in } \mathcal{O}(\Gamma), \quad \Gamma_{h/m}^{2 \rightarrow 1} = \Gamma_{h/m}^1, \quad \mathbf{n}_{\Gamma_{h/m}^{2 \rightarrow 1}} = \mathbf{n}_{\Gamma_{h/m}^1} \text{ on } \Gamma, \quad (16)$$

and

$$\mathbf{n}_{\Gamma_{h/m}^1} \rightarrow \mathbf{n}_\Gamma, \quad \Gamma_{h/m}^1 \rightarrow \Gamma \quad (17)$$

as one increases  $m$  even for fixed  $h$ .

---

<sup>1</sup>In [2] they use  $\mathbf{u} := \mathbf{P} \tilde{\mathbf{u}}$ , i.e.  $\mathbf{u} \neq \mathbf{u}^e$ . I prefer  $\mathbf{u} \equiv \mathbf{u}^e$  as in [1].

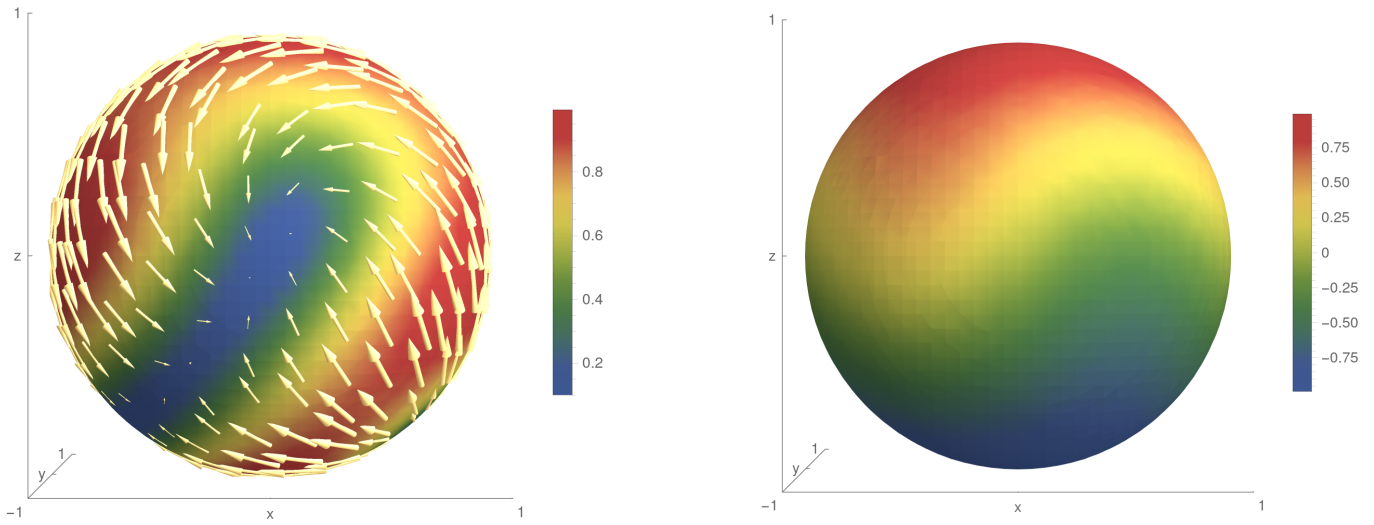


Figure 4: Exact velocity solution (Left) and pressure solution (Right) as in (15)

We have

$$\mathbf{n}_{\Gamma_{\text{sph}}}(\mathbf{x}) = \|\mathbf{x}\|^{-1} \mathbf{x} = \mathbf{n}_{\Gamma_{\text{sph}}}^e(\mathbf{x}), \quad (18)$$

$$\mathbf{P}_{\Gamma_{\text{sph}}}(\mathbf{x}) = \|\mathbf{x}\|^{-2} \begin{pmatrix} y^2 + z^2 & -xy & -xz \\ -xy & x^2 + z^2 & -yz \\ -xz & -yz & x^2 + y^2 \end{pmatrix} = \mathbf{P}_{\Gamma_{\text{sph}}}^e(\mathbf{x}), \quad (19)$$

$$\mathbf{H}_{\Gamma_{\text{sph}}}(\mathbf{x}) = \|\mathbf{x}\|^{-3} \begin{pmatrix} y^2 + z^2 & -xy & -xz \\ -xy & x^2 + z^2 & -yz \\ -xz & -yz & x^2 + y^2 \end{pmatrix} \neq \mathbf{H}_{\Gamma_{\text{sph}}}^e(\mathbf{x}) = \mathbf{P}_{\Gamma_{\text{sph}}}(\mathbf{x}). \quad (20)$$

We consider two choices for virtual refinement:  $m \propto h^{-1/2}$  and  $m \propto h^{-1}$ . The first choice assures  $h^3$ -accurate approximation of  $\Gamma$  and  $h^{3/2}$  accurate approximation of the normal vector, whereas the second choice assures  $h^4$ - and  $h^2$ -approximations. We refer to Figure 5.

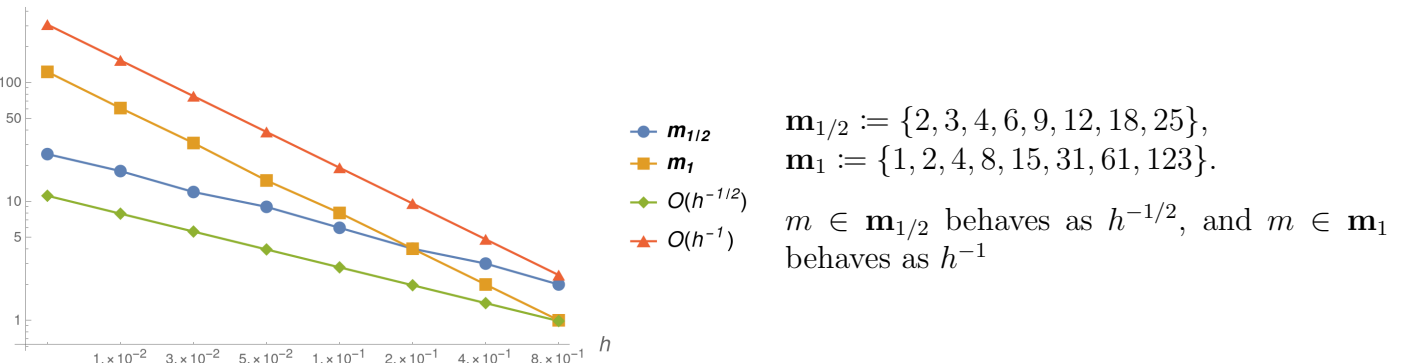


Figure 5: Virtual refinement parameter  $m$  for  $\Gamma_{h/m}^{2 \rightarrow 1}$

Table 1: Errors for normals and shape operator. Please see (16) and (17)

$m \in \mathbf{m}_{1/2}$ as in Figure 5					
$h$	$\ \mathbf{n}_\Gamma^e - \mathbf{n}_{\Gamma_h^2}\ _{\mathbb{L}^2(\Gamma_{h/m}^1)}$	$\ \mathbf{n}_\Gamma^e - \mathbf{n}_{\Gamma_{h/m}^1}\ _{\mathbb{L}^2(\Gamma_{h/m}^1)}$	Order	$\ \mathbf{H}_\Gamma^e - \mathbf{H}_{\Gamma_h^2}\ _{\mathbb{L}^2(\Gamma_{h/m}^1)}$	Order
$8.3 \times 10^{-1}$	$8.1 \times 10^{-16}$	$6.4 \times 10^{-1}$		$2.3 \times 10^{-1}$	
$4.2 \times 10^{-1}$	$1.1 \times 10^{-15}$	$2. \times 10^{-1}$	1.7	$2.5 \times 10^{-2}$	3.2
$2.1 \times 10^{-1}$	$2.3 \times 10^{-15}$	$7.6 \times 10^{-2}$	1.4	$3.5 \times 10^{-3}$	2.8
$1. \times 10^{-1}$	$5.2 \times 10^{-15}$	$2.5 \times 10^{-2}$	1.6	$3.9 \times 10^{-4}$	3.2
$5.2 \times 10^{-2}$	$9.3 \times 10^{-15}$	$8.4 \times 10^{-3}$	1.6	$4.3 \times 10^{-5}$	3.2
$2.6 \times 10^{-2}$	$1.9 \times 10^{-14}$	$3.1 \times 10^{-3}$	1.4	$6.1 \times 10^{-6}$	2.8
$1.3 \times 10^{-2}$	$3.6 \times 10^{-14}$	$1. \times 10^{-3}$	1.6	$6.8 \times 10^{-7}$	3.2

**2.2  $P_2 - P_1$  Trace FEM.** Next we compare inconsistent and consistent Trace FEM penalty formulations.

**2.2.1 Inconsistent penalty formulation.** We use the normal stabilization matrix  $\mathbf{C}_n$ . We stick to the approach (5), so with (16) we have

$$\begin{aligned}
\langle \mathbf{A} \vec{\mathbf{u}}, \vec{\mathbf{v}} \rangle &= \int_{\Gamma_{h/2}^1}^5 (2 E_{s,\Gamma}(\mathbf{u}) : E_{s,\Gamma}(\mathbf{v}) + \mathbf{u} \cdot \mathbf{v} + \tau (\mathbf{u} \cdot \mathbf{n}_\Gamma) (\mathbf{v} \cdot \mathbf{n}_\Gamma)) \, ds \\
&\quad + \rho_u \int_{\Omega_h^\Gamma}^5 \frac{\partial \mathbf{u}}{\partial \mathbf{n}_\Gamma} \cdot \frac{\partial \mathbf{v}}{\partial \mathbf{n}_\Gamma} \, dx, \quad \mathbf{A} \in \mathbb{R}^{n_A \times n_A}, \\
\langle \mathbf{B} \vec{\mathbf{u}}, \vec{\mathbf{q}} \rangle &= \int_{\Gamma_{h/2}^1}^5 \nabla_\Gamma q \cdot \mathbf{u} \, ds, \quad \mathbf{B} \in \mathbb{R}^{n_S \times n_A}, \\
\langle \mathbf{M}_0 \vec{\mathbf{p}}, \vec{\mathbf{q}} \rangle &= \int_{\Gamma_{h/2}^1}^5 p q \, ds, \quad \mathbf{M}_0 \in \mathbb{R}^{n_S \times n_S}, \\
\langle \mathbf{C}_n \vec{\mathbf{p}}, \vec{\mathbf{q}} \rangle &= \rho_p \int_{\Omega_h^\Gamma}^5 \frac{\partial p}{\partial \mathbf{n}_\Gamma} \frac{\partial q}{\partial \mathbf{n}_\Gamma} \, dx, \quad \mathbf{C}_n \in \mathbb{R}^{n_S \times n_S}.
\end{aligned} \tag{21}$$

Table 2: Convergence results.  $\tau = h^{-2}$ ,  $\rho_u = h$ ,  $\rho_p = h$ . Matrices are assembled as in (21)

$m \in \mathbf{m}_{1/2}$ as in Figure 5						
$h$	$\ \mathbf{u} - \mathbf{u}_h\ _{\mathbb{H}^1}$	Order	$\ \mathbf{u} - \mathbf{u}_h\ _{\mathbb{L}^2}$	Order	$\ p - p_h\ _{\mathbb{L}^2}$	Order
$8.3 \times 10^{-1}$	3.		1.8		2.1	
$4.2 \times 10^{-1}$	1.8	$7.4 \times 10^{-1}$	$9.1 \times 10^{-1}$	$9.7 \times 10^{-1}$	1.7	$2.7 \times 10^{-1}$
$2.1 \times 10^{-1}$	$7. \times 10^{-1}$	1.4	$3.4 \times 10^{-1}$	1.4	$6.9 \times 10^{-1}$	1.3
$1. \times 10^{-1}$	$2. \times 10^{-1}$	1.8	$9.9 \times 10^{-2}$	1.8	$2. \times 10^{-1}$	1.8
$5.2 \times 10^{-2}$	$5.2 \times 10^{-2}$	1.9	$2.6 \times 10^{-2}$	1.9	$5.2 \times 10^{-2}$	1.9
$2.6 \times 10^{-2}$	$1.3 \times 10^{-2}$	2.	$6.5 \times 10^{-3}$	2.	$1.3 \times 10^{-2}$	2.
$1.3 \times 10^{-2}$	$3.3 \times 10^{-3}$	2.	$1.6 \times 10^{-3}$	2.	$3.3 \times 10^{-3}$	2.

$h$	$\ \mathbf{u}_h \cdot \mathbf{n}\ _{\mathbb{L}^2}$	Order	Outer iterations	Residual norm
$8.33 \times 10^{-1}$	1.8		24	$6.2 \times 10^{-9}$
$4.17 \times 10^{-1}$	$9.2 \times 10^{-1}$	$9.4 \times 10^{-1}$	31	$5.4 \times 10^{-9}$
$2.08 \times 10^{-1}$	$3.5 \times 10^{-1}$	1.4	30	$9.8 \times 10^{-9}$
$1.04 \times 10^{-1}$	$9.9 \times 10^{-2}$	1.8	27	$7.8 \times 10^{-9}$
$5.21 \times 10^{-2}$	$2.6 \times 10^{-2}$	1.9	26	$8.3 \times 10^{-9}$
$2.6 \times 10^{-2}$	$6.5 \times 10^{-3}$	2.	26	$9.6 \times 10^{-9}$
$1.3 \times 10^{-2}$	$1.6 \times 10^{-3}$	2.	35	$7. \times 10^{-9}$

For statistics: using 64 CPUs, computation of the meshlevel 3 ( $h = 2.08 \times 10^{-1}$ ) takes  $\sim 1$  minute, meshlevel 4 takes  $\sim 7$  minutes, meshlevel 5 takes  $\sim 50$  minutes, meshlevel 6 takes 4.8 hours, and meshlevel 7 takes  $\sim 21.3$  hours.

**2.2.2 Consistent penalty formulation.** We consider the same formulation as in (21), but with the first  $\mathbf{A}_s$  term in the definition of  $\mathbf{A}$  changed according to (9). Thus with (16) we have

$$\langle \mathbf{A}_s \vec{\mathbf{u}}, \vec{\mathbf{v}} \rangle = \int_{\Gamma_{h/m}^1}^5 2(E_{s,\Gamma}(\mathbf{u}) - (\mathbf{u} \cdot \mathbf{n}_\Gamma) \mathbf{H}_\Gamma) : (E_{s,\Gamma}(\mathbf{v}) - (\mathbf{v} \cdot \mathbf{n}_\Gamma) \mathbf{H}_\Gamma) \, ds. \quad (22)$$

Table 4: Convergence results.  $\tau = h^{-2}$ ,  $\rho_u = h^{-1}$ ,  $\rho_p = h$ . Matrices are assembled as in (21)–(22)

$m \in \mathbf{m}_{1/2}$ as in Figure 5						
$h$	$\ \mathbf{u} - \mathbf{u}_h\ _{\mathbb{H}^1}$	Order	$\ \mathbf{u} - \mathbf{u}_h\ _{\mathbb{L}^2}$	Order	$\ p - p_h\ _{\mathbb{L}^2}$	Order
$8.3 \times 10^{-1}$	1.2		$4.8 \times 10^{-1}$		$4.2 \times 10^{-1}$	
$4.2 \times 10^{-1}$	$3.7 \times 10^{-1}$	1.8	$6.1 \times 10^{-2}$	3.	$1.1 \times 10^{-1}$	2.
$2.1 \times 10^{-1}$	$9.2 \times 10^{-2}$	2.	$5.8 \times 10^{-3}$	3.4	$2.5 \times 10^{-2}$	2.1
$1. \times 10^{-1}$	$2.2 \times 10^{-2}$	2.1	$5.6 \times 10^{-4}$	3.4	$6.3 \times 10^{-3}$	2.
$5.2 \times 10^{-2}$	$5.4 \times 10^{-3}$	2.	$5.2 \times 10^{-5}$	3.4	$1.7 \times 10^{-3}$	1.8
$2.6 \times 10^{-2}$	$1.4 \times 10^{-3}$	2.	$5.4 \times 10^{-6}$	3.3	$5.3 \times 10^{-4}$	1.7
$1.3 \times 10^{-2}$	$3.5 \times 10^{-4}$	2.	$6.9 \times 10^{-7}$	3.	$1.8 \times 10^{-4}$	1.6

$h$	$\ \mathbf{u}_h \cdot \mathbf{n}\ _{\mathbb{L}^2}$	Order	Outer iterations	Residual norm
$8.33 \times 10^{-1}$	$3.4 \times 10^{-1}$		26	$7.3 \times 10^{-9}$
$4.17 \times 10^{-1}$	$5.3 \times 10^{-2}$	2.7	33	$4.8 \times 10^{-9}$
$2.08 \times 10^{-1}$	$4.9 \times 10^{-3}$	3.4	31	$6. \times 10^{-9}$
$1.04 \times 10^{-1}$	$5. \times 10^{-4}$	3.3	27	$8.3 \times 10^{-9}$
$5.21 \times 10^{-2}$	$4.9 \times 10^{-5}$	3.4	26	$8.6 \times 10^{-9}$
$2.6 \times 10^{-2}$	$5. \times 10^{-6}$	3.3	26	$7.5 \times 10^{-9}$
$1.3 \times 10^{-2}$	$5.9 \times 10^{-7}$	3.1	34	$8. \times 10^{-9}$

For statistics: using 80 CPUs, computation of the meshlevel 7 ( $h = 1.3 \times 10^{-2}$ ) takes  $\sim 27$  hours with  $m = 18$  (computation also involves errors for normals and the shape operator).

### 3 Inf-sup stability: pressure Schur complement generalized eigenvalues

**3.1 Solution description.** We define matrices

$$\mathbf{C}_0 := \mathbf{0}, \quad \mathbf{M}_n := \mathbf{M}_0 + \mathbf{C}_n, \quad \mathbf{M}_{\text{full}} := \mathbf{M}_0 + \mathbf{C}_{\text{full}}. \quad (23)$$

We are interested in (generalized) extreme eigenvalues of the pressure Schur complement matrices

$$\mathbf{S}_0 := \mathbf{B} \mathbf{A}^{-1} \mathbf{B}^T, \quad \mathbf{S}_n := \mathbf{S}_0 + \mathbf{C}_n, \quad \mathbf{S}_{\text{full}} := \mathbf{S}_0 + \mathbf{C}_{\text{full}}, \quad (24)$$

i.e. in solving

$$\mathbf{S}_\star \mathbf{x} = \lambda \mathbf{M}_\star \mathbf{x}, \quad (25)$$

where “ $\star$ ” stands for “0,” “ $n$ ,” or “full.” We denote by  $0 = \lambda_1 < \lambda_2 \leq \dots \leq \lambda_{ns} = O(1)$  the spectrum of (25).

Computing  $\mathbf{A}^{-1}$  in (24) becomes troublesome already for  $h = 5.21 \times 10^{-2}$  ( $n_A = 32736$  for  $\mathbf{u} \in \mathbf{P}_1$  FE space): although  $\mathbf{A}$  is sparse,  $\mathbf{A}^{-1}$  is dense and consumes 8.5+ GB in double-precision arithmetic. A quick research showed that **Mathematica** has no built-in matrix-free eigenvalue routines. Intel MKL’s FEAST algorithm for computing (generalized) eigenvalues in an interval is suitable for matrix-free implementations; however, it requires some expensive operations to be implemented (e.g. matrix-matrix multiplications  $\mathbf{Y} \leftarrow \mathbf{S}_\star \mathbf{X}$ ,  $\mathbf{Y} \leftarrow \mathbf{M}_\star \mathbf{X}$  and approximating the action of inverses in the form  $\mathbf{y} \leftarrow (\sigma \mathbf{M}_\star - \mathbf{S}_\star)^{-1} \mathbf{x}$ ).

Taking this into account, instead of (25) we consider a perturbed<sup>2</sup> problem

$$\underbrace{\begin{bmatrix} \mathbf{A} & \mathbf{B}^T \\ \mathbf{B} & -\mathbf{C}_\star \end{bmatrix}}_{\mathcal{A}_\star :=} \begin{bmatrix} \mathbf{x} \\ \mathbf{y} \end{bmatrix} = \mu \underbrace{\begin{bmatrix} \epsilon \mathbf{A} & \\ & \mathbf{M}_\star \end{bmatrix}}_{\mathcal{M}_\star^\epsilon :=} \begin{bmatrix} \mathbf{x} \\ \mathbf{y} \end{bmatrix} \quad (26)$$

with  $0 < \epsilon \ll 1$ . For  $\mathcal{A}_0$  and  $\mathcal{M}_0^\epsilon$  we have

$$\mu = -\lambda + o(1) \quad \text{or} \quad \epsilon^{-1} + \lambda + o(1), \quad \epsilon \rightarrow 0. \quad (27)$$

This makes it easy to pick only “correct” eigenvalues. To ease the computation further we replace the  $(1, 1)$ -block of  $\mathcal{M}_\star^\epsilon$  with  $\epsilon \mathbf{I}$ .

To make sure that results are consistent we solve (26) for  $\epsilon = 10^{-5}$  and  $\epsilon = 10^{-6}$ ; for the coarse mesh levels we also check that the dense solver for (25) and the iterative one for (26) give solutions that coincide.

**3.2 Dependency of the spectrum on the mesh size.** Here we test inconsistent  $\mathbf{P}_1 - P_1$ , inconsistent  $\mathbf{P}_2 - P_1$ , and consistent  $\mathbf{P}_2 - P_1$  approaches.

Table 6: Spectrum of (25) for inconsistent  $\mathbf{P}_1 - P_1$ ,  $\tau = h^{-2}$ ,  $\rho_u = h$ ,  $\rho_p = h$ ,  $m \equiv 2$

$h$	$n_A$	$n_S$	$\Gamma = \Gamma_{\text{sph}}$					
			$\mathbf{S}_0$		$\mathbf{S}_n$		$\mathbf{S}_{\text{full}}$	
			$\lambda_2$	$\lambda_{ns}$		$\lambda_2$	$\lambda_{ns}$	
$8.33 \times 10^{-1}$	153	51	$1.32 \times 10^{-2}$	1.42	$7.48 \times 10^{-1}$	1.13	$9.58 \times 10^{-1}$	1.06
$4.17 \times 10^{-1}$	570	190	$5.12 \times 10^{-3}$	1.04	$5.77 \times 10^{-1}$	1.	$8.54 \times 10^{-1}$	1.
$2.08 \times 10^{-1}$	1992	664	$4.4 \times 10^{-3}$	$7.93 \times 10^{-1}$	$3.87 \times 10^{-1}$	1.	$6.71 \times 10^{-1}$	1.
$1.04 \times 10^{-1}$	8292	2764	$2.01 \times 10^{-3}$	$7.79 \times 10^{-1}$	$2.19 \times 10^{-1}$	1.	$5.82 \times 10^{-1}$	1.
$5.21 \times 10^{-2}$	32736	10912	$6.04 \times 10^{-5}$	$9.81 \times 10^{-1}$	$1.17 \times 10^{-1}$	1.	$5.37 \times 10^{-1}$	1.
$2.6 \times 10^{-2}$	131592	43864	$3.53 \times 10^{-5}$	$8.67 \times 10^{-1}$	$5.72 \times 10^{-2}$	1.	$5.16 \times 10^{-1}$	1.
$1.3 \times 10^{-2}$	525864	175288	$2.16 \times 10^{-6}$	$7.34 \times 10^{-1}$	$2.84 \times 10^{-2}$	1.	$5.04 \times 10^{-1}$	1.

<sup>2</sup>The majority of generalized eigenvalue solvers require left-hand-side matrix to be Hermitian and right-hand-side matrix to be Hermitian **positive definite**; that’s why we need to introduce  $\epsilon > 0$ .

$h$	$n_{\mathbf{A}}$	$n_{\mathbf{S}}$	$\Gamma = \Gamma_{\text{sph}}$					
			$\mathbf{S}_0$		$\mathbf{S}_n$		$\mathbf{S}_{\text{full}}$	
			$\lambda_2$	$\lambda_{ns}$	$\lambda_2$	$\lambda_{ns}$	$\lambda_2$	$\lambda_{ns}$
$2.08 \times 10^{-1}$	972	324	$5.04 \times 10^{-2}$	4.93	$2.84 \times 10^{-1}$	1.35	$3.64 \times 10^{-1}$	1.19
$1.04 \times 10^{-1}$	4740	1580	$2.99 \times 10^{-3}$	3.83	$1.58 \times 10^{-1}$	1.02	$3.35 \times 10^{-1}$	1.01
$5.21 \times 10^{-2}$	19704	6568	$1.11 \times 10^{-3}$	5.45	$7.73 \times 10^{-2}$	1.01	$3.25 \times 10^{-1}$	1.
$2.6 \times 10^{-2}$	80808	26936	$1.2 \times 10^{-4}$	5.42	$3.07 \times 10^{-2}$	1.01	$3.21 \times 10^{-1}$	1.
$1.3 \times 10^{-2}$	327036	109012	$1.77 \times 10^{-5}$	5.23	$1.18 \times 10^{-2}$	1.01	$3.16 \times 10^{-1}$	1.

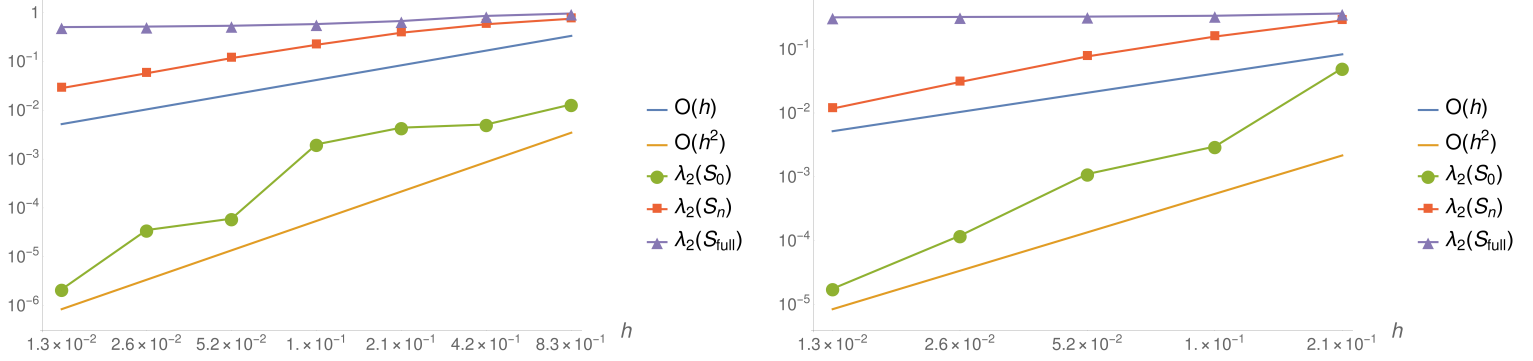


Figure 6: Log-log plot of  $\lambda_2$  for Tables 6?? (left) and 6?? (right)

Table 8: Spectrum of (25) for consistent  $\mathbf{P}_2 - P_1$ ,  $\tau = h^{-2}$ ,  $\rho_u = h^{-1}$ ,  $\rho_p = h$ ,  $m \in \mathbf{m}_{1/2}$  as in Figure 5

$h$	$n_{\mathbf{A}}$	$n_{\mathbf{S}}$	$\Gamma = \Gamma_{\text{sph}}$					
			$\mathbf{S}_0$		$\mathbf{S}_n$		$\mathbf{S}_{\text{full}}$	
			$\lambda_2$	$\lambda_{ns}$	$\lambda_2$	$\lambda_{ns}$	$\lambda_2$	$\lambda_{ns}$
$8.33 \times 10^{-1}$	789	51	$2.33 \times 10^{-1}$	1.07	$6.3 \times 10^{-1}$	1.	$8.81 \times 10^{-1}$	1.
$4.17 \times 10^{-1}$	3276	190	$4.72 \times 10^{-2}$	$6.97 \times 10^{-1}$	$5.29 \times 10^{-1}$	1.	$7.64 \times 10^{-1}$	1.
$2.08 \times 10^{-1}$	11718	664	$7.93 \times 10^{-2}$	$6.7 \times 10^{-1}$	$5.09 \times 10^{-1}$	1.	$6.39 \times 10^{-1}$	1.
$1.04 \times 10^{-1}$	48762	2764	$3.71 \times 10^{-2}$	$6.69 \times 10^{-1}$	$5.03 \times 10^{-1}$	1.	$5.73 \times 10^{-1}$	1.
$5.21 \times 10^{-2}$	193086	10912	$1.81 \times 10^{-3}$	$6.68 \times 10^{-1}$	$4.98 \times 10^{-1}$	1.	$5.36 \times 10^{-1}$	1.
$2.6 \times 10^{-2}$	775998	43864	$6.65 \times 10^{-4}$	$6.65 \times 10^{-1}$	$4.92 \times 10^{-1}$	1.	$5.17 \times 10^{-1}$	1.

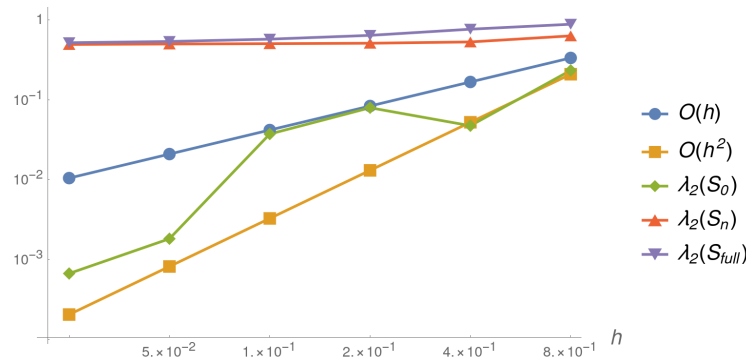


Figure 7: Log-log plot of  $\lambda_2$  for Table 8a

**3.3 Sensitivity of the spectrum to levelset shifts.** In this section we investigate the sensitivity of the spectrum to levelset shifts

$$\Gamma \mapsto \Gamma + \alpha \mathbf{s} \quad (28)$$

for some  $\alpha \in \mathbb{R}$  and  $\mathbf{s} \in \mathbb{R}^3$ ,  $\|\mathbf{s}\| = 1$ . We refer to Figure 8.

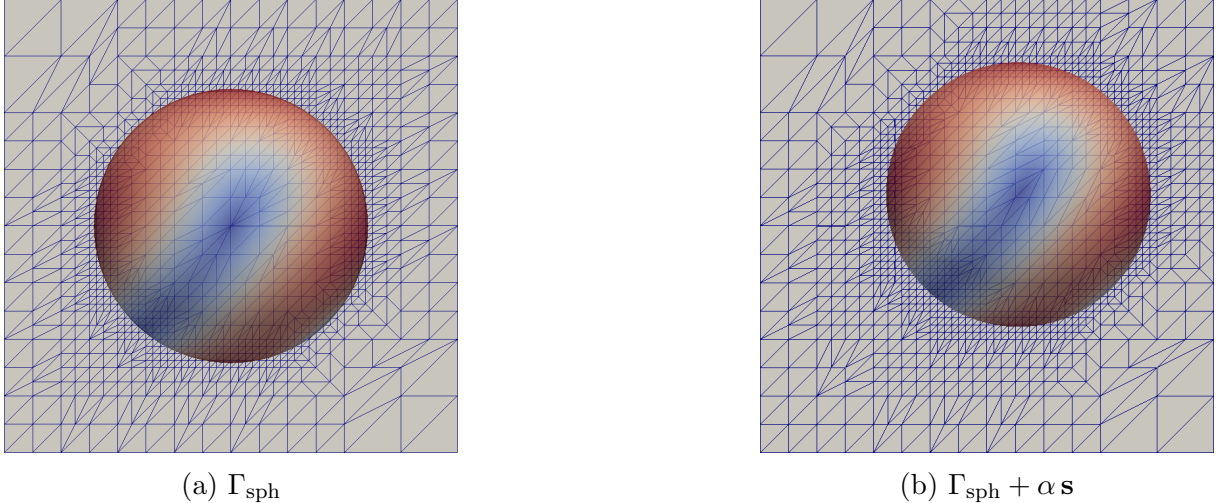


Figure 8:  $\|\mathbf{u}_h\|$  on the unit sphere (left) and the shifted unit sphere (right). Here  $\mathbf{s} = (1, 1, 1)^T/\sqrt{3}$ ,  $\alpha = 0.4$ , and  $h = 1.04 \times 10^{-1}$

Table 9: Spectrum of (25) for perturbed levelset  $\Gamma + \alpha \mathbf{s}$  for consistent  $\mathbf{P}_2 - P_1$ ,  $\tau = h^{-2}$ ,  $\rho_u = h^{-1}$ ,  $\rho_p = h$ ,  $m \in \mathbf{m}_{1/2}$  as in Figure 5. Here  $\mathbf{s} = (1, 1, 1)^T/\sqrt{3}$ ,  $h = 1.04 \times 10^{-1}$

Surface	$\mathbf{S}_0$		$\mathbf{S}_n$		$\mathbf{S}_{\text{full}}$	
	$\lambda_2$	$\lambda_{ns}$	$\lambda_2$	$\lambda_{ns}$	$\lambda_2$	$\lambda_{ns}$
$\Gamma_{\text{sph}} + 0.0 \mathbf{s}$	$3.714 \times 10^{-2}$	$6.69 \times 10^{-1}$	$5.03 \times 10^{-1}$	1.	$5.731 \times 10^{-1}$	1.
$\Gamma_{\text{sph}} + 0.1 \mathbf{s}$	$1.313 \times 10^{-3}$	$6.87 \times 10^{-1}$	$5.03 \times 10^{-1}$	1.	$5.733 \times 10^{-1}$	1.
$\Gamma_{\text{sph}} + 0.2 \mathbf{s}$	$1.248 \times 10^{-3}$	$6.7 \times 10^{-1}$	$5.03 \times 10^{-1}$	1.	$5.73 \times 10^{-1}$	1.
$\Gamma_{\text{sph}} + 0.3 \mathbf{s}$	$1.036 \times 10^{-2}$	$6.72 \times 10^{-1}$	$5.031 \times 10^{-1}$	1.	$5.73 \times 10^{-1}$	1.
$\Gamma_{\text{sph}} + 0.4 \mathbf{s}$	$5.315 \times 10^{-4}$	$6.72 \times 10^{-1}$	$5.031 \times 10^{-1}$	1.	$5.731 \times 10^{-1}$	1.

## References

- [1] T. Jankuhn and A. Reusken. Trace Finite Element Methods for Surface Vector-Laplace Equations. *arXiv e-prints*, April 2019.
- [2] M. Olshanskii, A. Quaini, A. Reusken, and V. Yushutin. A finite element method for the surface stokes problem. *SIAM Journal on Scientific Computing*, 40(4):A2492–A2518, 2018.